Available online at www.sciencedirect.com
SCIENCE DIRECT®
PERGAMON
International Journal of Heat and Mass Transfer 46 (2003) 4271–4277
International Journal of HEAT and MASS TRANSFER
www.elsevier.com/locate/ijhmt

Turbulent film condensation on a half oval body

Cha'o-Kuang Chen *, Hai-Ping Hu

Department of Mechanical Engineering, National Cheng Kung University, Tainan 70101, Taiwan, ROC

Received 11 November 2002; received in revised form 15 March 2003

Abstract

The paper is an investigation of turbulent film condensation on a half oval body. The high tangential velocity of the vapor flow at the boundary layer is determined from potential flow theory. The Colburn analogy is used to define the local liquid–vapor interfacial shear which occurs when the high velocity vapor flows across the body surface. The paper then presents a discussion of the results obtained for the local dimensionless film thickness and heat transfer characteristics. Furthermore, the present paper discusses the influence of Froude number, sub-cooling temperature and system pressure on mean Nusselt number.

Keywords: Turbulent; Film condensation; Oval

1. Introduction

Film condensation plays an important role in heat exchanger design, chemical engineering applications, electronic element cooling, and in the design of power plant cycles. Consequently, significant effort has been directed towards research into related fields. Many studies have been made on the laminar film condensation of a quiescent vapor on surface of various shapes since the pioneering work of Nusselt [1]. In 1966, Shekriladze et al. [2] analyzed film condensation on horizontal tubes under low velocity vapor flow conditions. Since then, much literature relating to researches into laminar film condensation on horizontal tubes has been published, e.g. Refs. [3–5]. Yang and Hsu [6] analyzed the problem of combined free- and forced-convection on a horizontal elliptical tube, and paid particular attention to the effects of vapor shear and pressure gradient.

Studies of the heat transfer process often consider the case of a spherical body. Typical studies include those conducted by Yang [7] and Karimi [8], which both considered the case of an isothermal wall with natural convection condensation. The case of forced-convection film condensation on a sphere using constant properties analysis has also been investigated, e.g. by Hu and Jacobi [9]. Furthermore, in 1992, Jacobi [10] analyzed the filmwise condensation from a flowing vapor onto isothermal, axisymmetric bodies with the model of Dhir and Lienhard [11].

From the above, it will be clear that there has been significant discussion of laminar film condensation within published literature. However, it is also worthwhile developing an understanding of turbulent flow condensation. At first, in the research of Michael et al. [12] in 1989, the authors pointed out that condensate films may be partially turbulent at high vapor velocities. According to the statement, Sarma et al. [13] carried out theoretical research into turbulent film condensation on a horizontal tube, and found that his results were in good agreement with experimental data relating to the condensation of steam flowing under a turbulent regime. However, there has been relatively little recent investigation of the issues relating to turbulent film condensation on a half oval body e.g. the relationships between the various heat transfer characteristics of the condensation film. Therefore, the aim of this present study is to investigate turbulent film condensation on a half oval body employing the model of Sarma et al. We hope that

* Corresponding author. Tel.: +886-6-2757575x62140; fax: +886-6-2342081.
E-mail address: ckchen@mail.ncku.edu.tw (C.-K. Chen).

0017-9310/$ - see front matter © 2003 Elsevier Ltd. All rights reserved.
doi:10.1016/S0017-9310(03)00150-9

Nomenclature

a	radial of nose
C_p	specific heat of condensate at constant pressure
f	average friction coefficient
Fr	Froude number, u_∞^2/ga
Gr	Grashof number, ga^3/v_l^2
g	acceleration due to gravity
h	local heat transfer coefficient
h_{fg}	latent heat of condensate
k	thermal conductivity
Nu	Nusselt number
P	system pressure parameter
Pr	Prandtl number
Re	Reynolds number
Re^+	shear Reynolds
Re^*	wall shear Reynolds parameter
S	sub-cooling parameter, $C_p(T_s - T_w)/h_{fg}Pr$
T	temperature
T^+	dimensionless temperature
u	velocity component in x-direction
u_e	the tangential vapor velocity at the edge of the boundary layer
u^*	shear velocity
u^+	dimensionless velocity
x	streamwise boundary-layer coordinate
y	transverse boundary-layer coordinate
y^+	dimensionless distance

Greek symbols

δ	condensate film thickness
δ^+	dimensionless film thickness
ϕ	interfacial shear parameter
v	kinematic viscosity
ρ	density
τ	shear stress
∞	in the free stream
ε	eddy diffusivity

Subscripts

sat	saturation
v	vapor
l	liquid
w	oval wall
δ	vapor–liquid interface

the present study can be applied to design a reflux condenser for a centrifuge boiling.

2. Analysis

This paper considers a half oval body, whose uniform wall surface temperature is represented by T_w, immersed in a downward and pure vapor flow at its saturation temperature, T_{sat}, moving at a uniform velocity, u_∞. Steady-state condensation occurs on the wall of the body, and a continuous film of the liquid runs downward over its surface. The physical model and the coordinate system adopted in this study are shown in Fig. 1.

If turbulent flow occurs near the wall of the body surface, then it may be assumed that the thickness of the liquid film is much smaller than the radial of nose. It is possible to make the assumption that it is sufficiently close to the wall that the inertial force may be neglected. Since the condensate film is turbulent at the high vapor velocity, the surface tension effect may be neglected. Furthermore, it is assumed that the condensate film is under a turbulent region in all regions other than at the upper stagnation point. Vapor boundary layer separation of vapor around the condensation film is neglected. These assumptions allow the force balance equation to be expressed in the following equation:

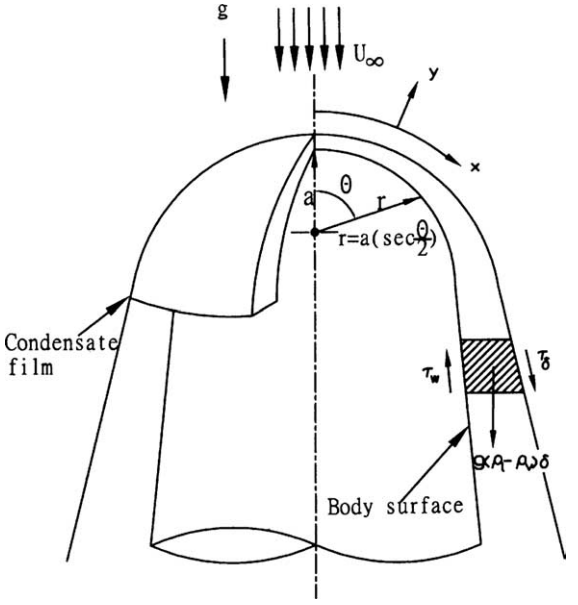

Fig. 1. Physical model and coordinate system.

$$\tau_w - \tau_\delta - g\delta(\rho_l - \rho_v)\sin\theta = 0 \tag{1}$$

where the wall shear stress

$$\tau_w = \rho(v + \varepsilon_m)\frac{du}{dy} \tag{2}$$

Thus, the force balance for an element of the condensate film (refer to Fig. 1) is governed by the wall stress, the body force and the liquid–vapor interface shear stress. The limitation of the Eq. (1) is condensation occurs only under the condition of lower condensation rate, i.e. sub-cooling parameter is a low value.

Owing to all the heat conducted across the film is a result of the condensation of the vapors at the interface; the energy balance equation of the condensate film can be expressed as

$$\frac{\rho_l}{\sec\frac{\theta}{2}}\frac{d}{dx}\int_0^{\delta}\sec\frac{\theta}{2}u\,dy=\frac{K_l}{h_{fg}}\frac{dT}{dy}_{y=0} \tag{3}$$

With reference to Fig. 1 the differential arc length may be written as

$$dx=a\sec\frac{\theta}{2}\sqrt{1+\frac{1}{2}\sin\frac{\theta}{2}}d\theta \tag{4}$$

Assuming that the flow is sufficiently close to the wall. The influence of turbulent conduction across the condensate layer is more significant that the influence of convection. Therefore, the energy equation can be expressed as [14]:

$$\frac{d}{dy}\left[\left(1+\frac{\varepsilon_H}{v}Pr\right)\frac{dT}{dy}\right]=0 \tag{5}$$

The boundary conditions are described as

$$\begin{aligned}&(1)\quad \text{at } y=0;\quad T=T_w\\&(2)\quad \text{at } y=\delta;\quad T=T_{sat}\end{aligned} \tag{6}$$

In the high vapor velocity, the semi-empirical equation that describes heat transfer in the flow parallel to a moderately curved surface may also be used to describe the heat transfer in the flow on an oval body. Jakob [15] proposed that this situation might be described by the following expression:

$$Nu=0.034Re^{4/5}Pr^{1/3} \tag{7}$$

The limitation of Eq. (7) is that it excludes from using liquid metals.

According to Colburn analogy the heat transfer factor can be represented as follows:

$$\frac{f}{2}=StPr^{2/3} \tag{8}$$

where

$$St=\frac{Nu}{RePr}$$

The average friction coefficient may then be written as

$$f=\frac{\int_0^{\frac{5}{6}\pi}f_\theta 2\pi a^2\sin\theta\sec^2\frac{\theta}{2}\sqrt{1+\frac{1}{2}\sin\frac{\theta}{2}}d\theta}{\int_0^{\frac{5}{6}\pi}2\pi a^2\sin\theta\sec^2\frac{\theta}{2}\sqrt{1+\frac{1}{2}\sin\frac{\theta}{2}}d\theta} \tag{9}$$

Combining Eqs. (7)–(9) yields an expression for the local friction coefficient, i.e.

$$f_\theta=CRe_v^{-0.2}\sin\theta \tag{10}$$

where the value of constant C is 0.079, $Re_v=2u_\infty a/v_v$.

The local shear stress is defined by the relationship:

$$\tau_\delta=\tfrac{1}{2}\rho_v u_v^2 f_\theta \tag{11}$$

In the description of potential flow theory about Rankine half body of revolution, the tangential velocity is given by

$$u_e^2=u_\infty^2\left(1-2\cos\theta\cos^2\frac{\theta}{2}+\cos^4\frac{\theta}{2}\right) \tag{12}$$

Combining Eqs. (10)–(12) allows the local shear stress to be expressed as

$$\tau_\delta=C\rho_v u_\infty^2 Re_v^{-0.2}\left(1-2\cos\theta\cos^2\frac{\theta}{2}+\cos^4\frac{\theta}{2}\right)\sin\theta \tag{13}$$

Incorporating the interfacial vapor shear stress, τ_δ, given by Eq. (13) into the elemental force balance enables Eq. (1) to be rewritten in the following form:

$$\tau_w=C\rho_v u_\infty^2 Re_v^{-0.2}\left(1-2\cos\theta\cos^2\frac{\theta}{2}+\cos^4\frac{\theta}{2}\right)\sin\theta+g\delta(\rho_l-\rho_v)\sin\theta \tag{14}$$

The following dimensionless variables and equations are now defined:

$$\begin{aligned}&\text{friction velocity}\quad u^*=\left(\frac{\tau_w}{\rho}\right)^{1/2}\\&\text{dimensionless velocity}\quad u^+=\frac{u}{u^*}\\&\text{dimensionless temperature}\quad T^+=\frac{T-T_w}{T_{sat}-T_w}\\&\text{dimensionless distance}\quad y^+=\frac{yu^*}{v_l}\\&\text{dimensionless thickness}\quad \delta^+=\frac{\delta u^*}{v_l}\\&\text{wall shear Reynolds parameter}\quad Re^*=\frac{Re^+}{Gr^{1/3}}\\&\text{shear Reynolds}\quad Re^+=\frac{au^*}{v_l}\\&\text{Froude number}\quad Fr=\frac{u_\infty^2}{ga}\\&\text{modified Grashof number}\quad Gr=\frac{ga^3}{v_l^2}\frac{\rho_l-\rho_v}{\rho_l}\\&\text{sub-cooling parameter}\quad S=\frac{C_p(T_{sat}-T_w)}{h_{fg}Pr}\end{aligned} \tag{15}$$

The eddy diffusivity for momentum ε_M is assumed to be equal to that for energy ε_H. Substitution of these

variables into the energy equation (Eq. (5)) yields the following dimensionless energy equation:

$$\frac{\mathrm{d}}{\mathrm{d}y^+}\left[\left(1+\frac{\varepsilon_\mathrm{m}}{\nu_\mathrm{l}}Pr\right)\frac{\mathrm{d}T^+}{\mathrm{d}y^+}\right]=0 \tag{16}$$

The dimensionless boundary conditions of Eq. (16) are as follows:

$$\begin{aligned}&(1)\quad \text{at } y^+=0;\quad T^+=0\\ &(2)\quad \text{at } y^+=\delta^+;\quad T^+=1\end{aligned} \tag{17}$$

Substitution of Eq. (15) into Eqs. (3) and (14) gives

$$\frac{\mathrm{d}}{\sec\frac{\theta}{2}\,\mathrm{d}\theta}\int_0^{\delta^+}\sec\frac{\theta}{2}u^+\,\mathrm{d}y^+ = S\,Gr^{1/3}\sec\frac{\theta}{2}\sqrt{1+\frac{1}{2}\sin\frac{\theta}{2}}Re^*\left.\frac{\mathrm{d}T^+}{\mathrm{d}y^+}\right|_{y^+=0} \tag{18}$$

$$Re^{*3}=Re^*C2^{-0.2}\frac{\rho_\mathrm{v}}{\rho_\mathrm{l}}\left(\frac{\nu_\mathrm{l}}{\nu_\mathrm{v}}\right)^{-0.2}Gr^{1.4/6}Fr^{0.9}\times\left(1-2\cos\theta\cos^2\frac{\theta}{2}+\cos^4\frac{\theta}{2}\right)\sin\theta+\delta^+\sin\theta \tag{19}$$

where $C2^{-0.2}\frac{\rho_\mathrm{v}}{\rho_\mathrm{l}}\left(\frac{\nu_\mathrm{l}}{\nu_\mathrm{v}}\right)^{-0.2}Gr^{1.4/6}$ is defined as the interfacial shear parameter ϕ.

Further, the velocity profile of Eq. (18) can be obtained from the following expression [14]:

$$\left(1+\frac{\varepsilon_\mathrm{m}}{\nu}\right)\frac{\mathrm{d}u^+}{\mathrm{d}y^+}=1 \tag{20}$$

The boundary condition of Eq. (20) is

$$u^+=0\quad\text{at } y^+=0 \tag{21}$$

The eddy diffusivity distribution relevant to the present study, was presented by Kato et al. [16], and is given by the following equation:

$$\frac{\varepsilon_\mathrm{m}}{\nu}=0.4y^+[1-\exp(-0.0017y^{+2})] \tag{22}$$

Substituting the Eqs. (20)–(22) into Eq. (16) yields the following equation:

$$\left.\frac{\mathrm{d}T^+}{\mathrm{d}y^+}\right|_{y^+=0}=\frac{1}{\displaystyle\int_0^{\delta^+}\frac{\mathrm{d}y^+}{1+0.4y^+[1-\exp(-0.0017y^{+2})]Pr}\;\;1+0.4y^+[1-\exp(-0.0017y^{+2})]Pr} \tag{23}$$

Substitution of Eq. (20) into Eq. (18) gives the following expression:

$$Re^*=\frac{\frac{\mathrm{d}}{\mathrm{d}\theta}\int_0^{\delta^+}\sec\frac{\theta}{2}u^+\,\mathrm{d}y^+}{S\,Gr^{1/3}\sec^2\frac{\theta}{2}\sqrt{1+\frac{1}{2}\sin\frac{\theta}{2}}\left.\frac{\mathrm{d}T^+}{\mathrm{d}y^+}\right|_{y^+=0}} \tag{24}$$

Rewriting Eq. (19), gives the local dimensionless thickness as

$$\delta^+=\frac{Re^{*3}-Re^*\phi Fr^{0.9}\left(1-2\cos\theta\cos^2\frac{\theta}{2}+\cos^4\frac{\theta}{2}\right)\sin\theta}{\sin\theta} \tag{25}$$

Considering the condensation heat transfer, interpreting the results of the model is straightforward if the following heat transfer coefficient is adopted:

$$K_\mathrm{l}\left.\frac{\partial T}{\partial y}\right|_{y=0}=h(T_\mathrm{s}-T_\mathrm{w}) \tag{26}$$

In a dimensionless form, Eq. (26) can be written as follow:

$$Nu=Re^+\left.\frac{\mathrm{d}T^+}{\mathrm{d}y^+}\right|_{y^+=0} \tag{27}$$

Obviously, the local Nusselt number can also be expressed as follows:

$$\frac{Nu}{Re_\mathrm{l}^{1/2}}=\frac{Gr^{1/12}}{Fr^{1/4}}Re^*\left.\frac{\mathrm{d}T^+}{\mathrm{d}y^+}\right|_{y^+=0} \tag{28}$$

where $Re_\mathrm{l}=u_\infty a/\nu_\mathrm{l}$ and $Nu=ha/k_\mathrm{l}$.

Thus, one can obtain the mean Nusselt number from Eq. (28) as follows:

$$\frac{Nu_\mathrm{m}}{Re^{1/2}}=\frac{1}{2\pi}\int_0^{\frac{5}{6}\pi}\frac{Nu}{Re^{1/2}}\frac{\sin\theta}{\cos^2\frac{\theta}{2}}\sqrt{1+\frac{1}{2}\sin\frac{\theta}{2}}\mathrm{d}\theta \tag{29}$$

The equations developed above will now be applied in the following section of this paper, which relates to a numerical method.

3. Numerical method

The dimensionless governing equations (23)–(25) can be used to estimate the values of δ^+ and Re^*. The estimation process can be described as follows:

(1) Boundary conditions corresponding to the system conditions are input; i.e. at $i=0$, the dimensionless film thickness δ^+ is zero. At the next node, i.e. $i=i+1$, the value of θ is given by $\theta_{i+1}=\theta_i+\Delta\theta$, where $\Delta\theta=(\pi/300)$.
(2) In Eq. (23), the dimensionless film thickness is assumed to be $\delta_{i=1}^{+Z}$ at the first node, i.e. $i=1$. The temperature gradient $(\mathrm{d}T^+/\mathrm{d}y^+)_{y^+=0}$ can be calculated and then substituted into Eq. (24).
(3) The shear Reynolds parameter at the first node $(Re_{i=1}^*)$ can be calculated.
(4) Substitution of the shear Reynolds parameter, Re^*, into Eq. (25) allows a new value of the dimensionless film thickness to be determined, i.e. $\delta_{i=1}^{+Z+1}$. If comparison of $\delta_{i=1}^{+Z}$ and $\delta_{i=1}^{+Z+1}$ reveals no similarity between

the two values, a new, corrected value of $\delta_{i=1}^{+Z}$ will be assumed, and computation continues until the convergence criterion is attained, i.e.

$$\left|\frac{\delta_i^{+Z+1}-\delta_i^{+Z}}{\delta_i^{+Z+1}}\right| \leqslant 1\times 10^{-6}$$

(5) This process is repeated at the next node position, i.e. $\theta_{i+1}=\theta_i+\Delta\theta$. Because numeric shows an infinite value when $\theta=\pi$, all nodes are within the range $0<\theta\leqslant\frac{5}{6}\pi$.
(6) The local Nusselt number and the mean Nusselt number are then calculated.
(7) Set angular parameter $\theta^+=\frac{\theta}{5\pi/6}$.

4. Results and discussion

Fig. 2 presents the variation of the dimensionless film thickness of the condensate along the surface of the half body for different values of the sub-cooling parameter, S. At the upper stagnation point ($\theta^+=0$), the value of the dimensionless film thickness, δ^+, is zero. Observation of Fig. 2 shows that the dimensionless film thickness increases continuously as the value of θ^+ increases, i.e. from its minimum value at the upper stagnation point to a maximum value at the trailing edge (i.e. $\theta^+=1$). Furthermore, it can be seen that an increase in both Froude number and sub-cooling parameter leads to an increase in the local condensate film thickness.

Fig. 3 plots data derived from Eq. (27) to present the variation of the local Nusselt number of the condensate along the body surface for three sub-cooling parameter values. It is seen that the value of the shear Reynolds (Re^*) parameter gradually increases from its minimum value at the upper stagnation point for increasing angular positions, and that it reaches a peak value about at $\theta^+=1/2$. After this point, the value of the shear Reynolds parameter then gradually decreases, and reaches a lower value at the trailing edge. Fig. 3 also shows quite clearly that the local Nusselt numbers decrease as the value of the sub-cooling parameter increases.

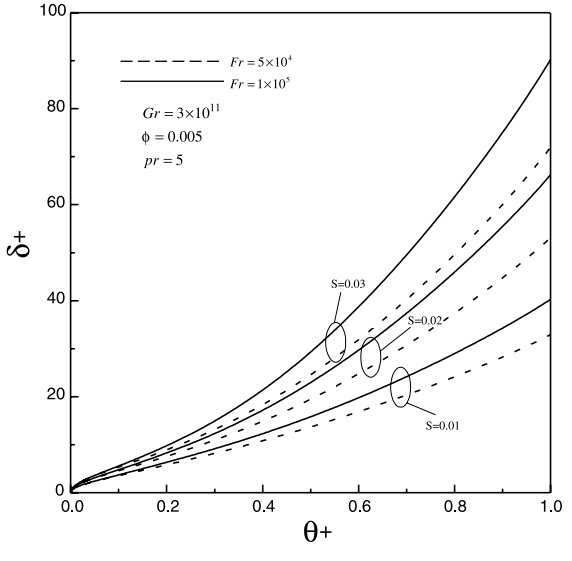

Fig. 2. Variation of dimensionless local film thickness with angle parameter, $\theta^+=\theta/(\frac{5\pi}{6})$.

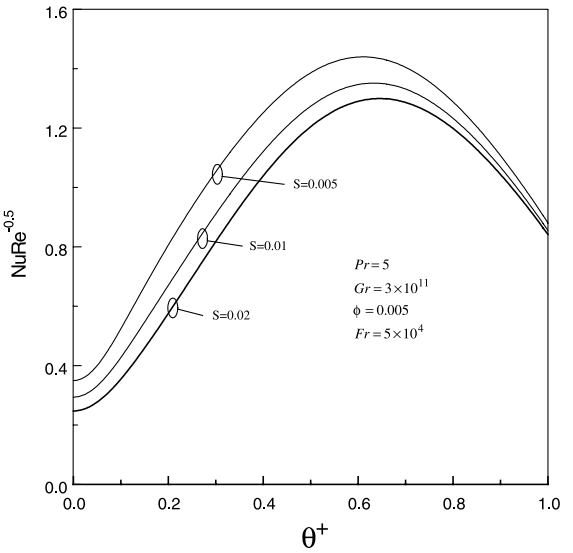

Fig. 3. Variation of local Nusselt number with angle parameter.

Fig. 4 presents the relationship between the mean Nusselt number of the half body and the sub-cooling parameter for different Froude numbers. For any given Froude number, it can be seen that the mean Nusselt number increases as the value of the sub-cooling parameter, S, decreases. However, for any given value of S, the mean Nusselt number is dependent upon the Froude number and it is seen to increase as the Froude number increases.

Fig. 5 shows the influence of the shear parameter on the mean Nusselt value for three different Fr values. The system pressure parameter is given by $p=\rho_v Pr/\rho_l Ja$, thus, when ρ_v/ρ_l is higher, (P·S) is also higher (where $S=Ja/Pr$). Observation of the figure shows that for a fixed value of S, the system pressure increases as the value of ϕ increases. As a result, the increase in system pressure leads to an increase in the mean Nusselt number.

Fig. 6 shows the influence of the system pressure on the mean Nusselt number for three different values of the sub-cooling parameter, S, within the values of 0.005, 0.01 and 0.02. It can be seen that the mean Nusselt number decreases as the value of S increases.

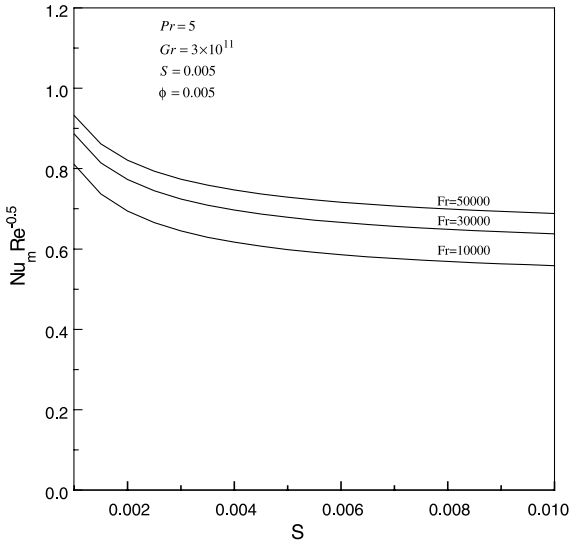

Fig. 4. Effect of sub-cooling parameter on mean Nusselt number.

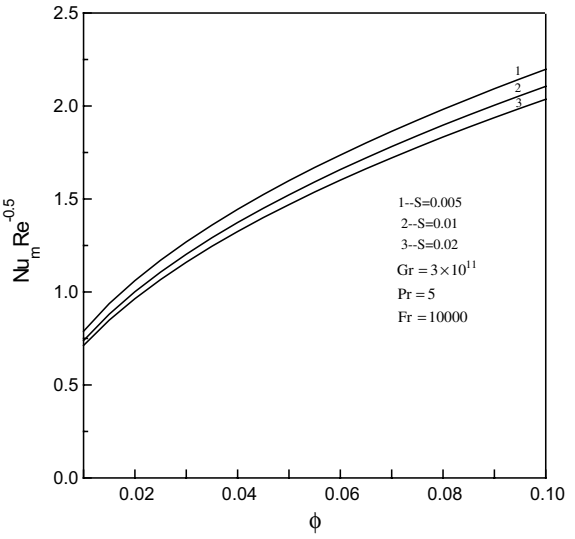

Fig. 6. Variation of mean Nusselt number with ϕ for different sub-cooling.

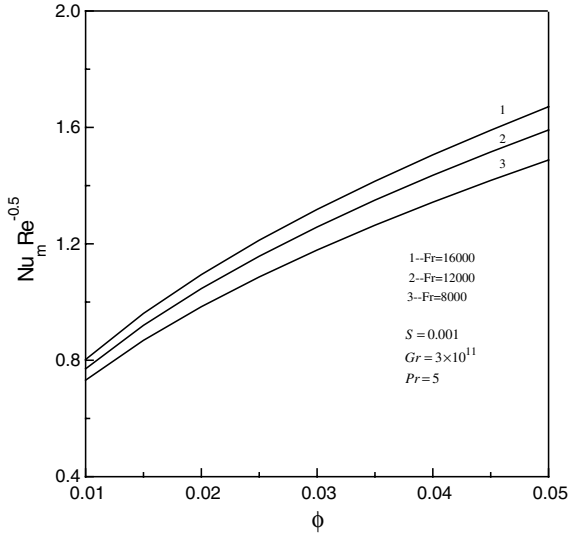

Fig. 5. Effect of interfacial parameter on mean Nusselt number for different Fr.

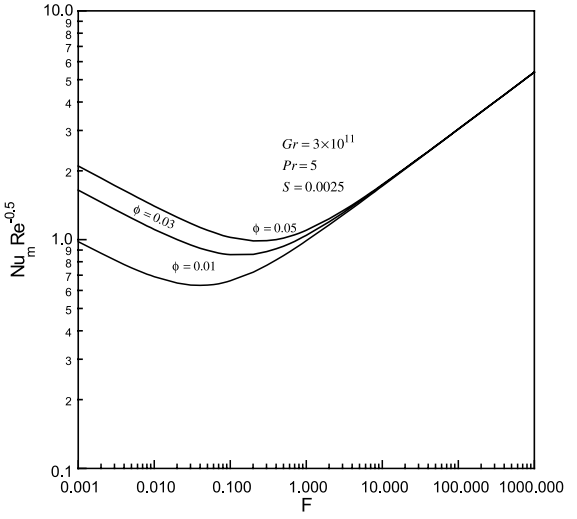

Fig. 7. Dependence of mean Nusselt number on F value, $F = 2/(FrS)$.

Additionally, it is noted that an increase in system pressure results in an increase in the mean Nusselt number.

Fig. 7 shows the effect of the F-value on the mean Nusselt number. In the case of low vapor velocity (i.e. $F > 10$), the results of the present study are tend to blend with the free film condensation mode. However, when the value of F decreases and tends toward zero, the results for the mean Nusselt number resemble the case of forced film condensation. The figure also indicates that as the value of F decreases, the mean Nusselt number will transfer from a free- to a forced-condensation mode earlier when the system pressure is higher. It is also noted that an increase in system pressure brings about an increase in the mean Nusselt number. Such a phenomenon is particularly apparent in forced film condensation conditions. The difference in the relationship between the Nusselt number and ϕ in high and low vapor velocity regions is not unexpected "because of the onset of turbulence in the condensate film" in the high vapor velocity region [17].

5. Conclusions

The following conclusions may be drawn from the results of this study:

(1) The limitations on the expression are: that radial of nose greatly exceeds the film thickness, that the condensate film occurs only under the condition of lower condensation rate, and that liquid metals are excluded.
(2) A larger sub-cooling parameter will increase the condensate film thickness; however, the increase of sub-cooling parameter will decrease the heat transfer coefficient.
(3) Both increase Froude and system pressure will increase the average heat transfer.
(4) In the case of low vapor velocity (i.e. $F > 10$), the results of the present study are tend to blend with the free film condensation mode. When the value of F decreases, the mean Nusselt number will transfer from a free- to a forced-condensation mode earlier when the system pressure is higher. Furthermore, in the case of high vapor velocity, the mean Nusselt number is much more dependent upon the system pressure, "because of the onset of turbulence in the condensate film" [17] in the high vapor velocity region.

References

[1] W. Nusselt, Die oberflachen kondensation des wasserdampers, Zeitsehrift desvereines deutsher ingenieure 60 (1916) 541–546.
[2] I.G. Shekriladze, V.I. Gomelauri, Theoretical study of laminar film condensation of flowing vapor, Int. J. Heat Mass Transfer 9 (1966) 581–591.
[3] T. Fujii, H. Uehara, C. Kurata, Laminar filmwise condensation of flowing vapor on a horizontal condenser, Int. J. Heat Mass Transfer 15 (1972) 235–246.
[4] T. Fujii, H. Honda, K. Oda, Condensation of steam on a horizontal tube the influence of oncoming velocity and thermal condition at the tube wall, Condensation Heat transfer, ASME, 18th National Heat Transfer Conference, San Diego, 1979, pp. 35–43.
[5] H. Honda, S. Zozu, B. Uchima, T. Fujii, Effect of vapor velocity on film condensation of R-113 on horizontal tubes in across flow, Int. J. Heat Mass Transfer 29 (3) (1986) 429–438.
[6] S.A. Yang, C.H. Hsu, Free- and forced-convection film condensation from a horizontal elliptic tube with a vertical plate and horizontal tube as special cases, Int. J. Heat Fluid Flow 18 (1997) 567–574.
[7] J.W. Yang, Laminar film condensation on a sphere, ASME J. Heat Transfer 95 (C) (1977) 174–178.
[8] A. Karimi, Laminar film condensation on helical reflux condensers and related configurations, Int. J. Heat Mass Transfer 20 (1977) 1137–1144.
[9] H. Hu, A.M. Jacobi, Vapor shear and pressure gradient effects during filmwise condensation from a flowing vapor onto a sphere, Exp. Therm. Fluid Sci. 5 (1992) 548–555.
[10] A.M. Jacobi, Filmwise condensation from a flowing vapor onto isothermal, axisymmetric bodies, J. Thermophys. Heat Transfer 6 (1992) 321–325.
[11] V. Dhir, J. Lienhard, Laminar film condensation on plane and axisymmetric bodies in nonuniform gravity, ASME J. Heat Transfer 93 (1971) 97–100.
[12] A.G. Michael, J.W. Rose, L.C. Daniels, Forced convection condensation on a horizontal tube—experiments with vertical downflow of steam, ASME J. Heat Transfer 111 (1989) 792–797.
[13] P.K. Sarma, B. Vijayalakshmi, F. Mayinger, S. Kakac, Turbulent film condensation on a horizontal tube with external flow of pure vapors, Int. J. Heat Mass Transfer 41 (1998) 537–545.
[14] A. Bejan, Convection Heat Transfer, Wiley, New York, 1995.
[15] M. Jakob, Heat Transfer, Wiley, New York, 1955.
[16] H. Kato, N.N. Shiwaki, M. Hirota, On the turbulent heat transfer by free convection from a vertical plate, Int. J. Heat Mass Transfer 11 (1968) 117–1125.
[17] W.C. Lee, S. Rahbar, J.W. Rose, Film condensation of refrigerant 113 and ethanediol on a horizontal tube—effect of vapor velocity, ASME J. Heat Transfer 106 (1984) 524–530.